

Spin Conductance in one-dimensional Spin-Phonon systems

Kim Louis and Xenophon Zotos

*Department of Physics, University of Crete and Foundation for Research and Technology-Hellas,
P. O. Box 2208, 71003 Heraklion, Crete, Greece*

(Dated: November 15, 2018)

We present results for the spin conductance of the one dimensional spin-1/2 Heisenberg and XY model coupled to phonons. We apply an approach based on the Stochastic Series Expansion (Quantum Monte Carlo) method to evaluate the conductance for a variety of phonon dispersions and values of spin-phonon coupling. From our numerical simulations and analytical arguments, we derive several scaling laws for the conductance.

PACS numbers: 75.30.Gw,75.10.Jm,78.30.-j

Introduction — Controlling and understanding the dynamics and transport of spins is an experimental and theoretical challenge aiming at the development of mesoscopic systems for spintronics applications. In particular, the interest is recently focusing on the effect of interactions and the coupling of spin systems to the environment; several proposals for the generation and detection of spin currents exist.¹ As a key quantity characterizing ballistic mesoscopic spin transport is the (spin) conductance, it is important to understand its behavior in prototype interacting spin systems coupled to lattice vibrations – phonons.

Related to this problem, since the 60's, the spin-Peierls transition, the dimerization of a lattice due to the spin-phonon interaction in the bulk, has been discussed for quasi-one dimensional compounds as TTF, TCNQ, CuGeO_3 . A variety of analytical and numerical methods are still employed in the study of the dependence of the transition on the phonon spectrum and spin-phonon coupling.^{2,3}

Finally, in close relation to this work, spurred by the experimental finding of an exceptionally high thermal conductivity^{4,5} in quasi-one dimensional transition metal compounds, there is recently considerable experimental and theoretical research interest in the finite temperature transport properties of spin models.^{6,7,8} In particular, this activity leads to the development of novel numerical simulation techniques⁹ for the calculation of zero and finite temperature transport properties in one dimensional electronic/spin models.

In this paper we address the fundamental question of the spin conductance of the spin-1/2 Heisenberg model and the XY model coupled to phonons. Thus this study, on the one hand, sheds light from a new perspective on the old question of the spin-Peierls transition and on the other hand addresses a prototype question in mesoscopic physics; it is of direct experimental relevance, as a detailed experimental set-up for the observation of the spin conductance was recently proposed.¹⁰

Quantum Monte Carlo (QMC) methods have already been successfully applied to the evaluation of thermodynamic quantities in spin-phonon systems.^{3,11,12} We will use here the Stochastic Series Expansion (SSE) which allows the calculation of the conductance of interacting

spin systems;⁹ in this original application we extend it to coupled spin-phonon systems.

In the following we will first discuss the model and the method we are using, then we will present data for the conductance in the Heisenberg model for optical and acoustic phonon dispersions, and derive several scaling laws. Finally, we will show results for the XY model coupled to optical phonons.

Model and method — The nominal spin-Peierls Hamiltonian describing the coupling of the one dimensional Heisenberg model to lattice vibrations is given by

$$H = \sum_n [J + \lambda(x_n - x_{n+1})] (\mathbf{S}_n \cdot \mathbf{S}_{n+1}) + \sum_n \omega_0/2 [2p_n^2 + (x_n - x_{n+1})^2], \quad (1)$$

where \mathbf{S}_n are spin-1/2 operators and x_n, p_n the displacement and momentum operators of the ions (ω_0 is the characteristic phonon frequency and here we set $\hbar = 1$).

Because of the minus sign problem, this system eludes a direct analysis using the QMC method that we intend to employ here. Hence, we resort to the following generalized Hamiltonian which is an extension of the Hamiltonian discussed in Refs. 3,11,

$$H = \sum_{n=0}^{N-1} \left(\tilde{J} + \alpha_1(a_n + a_n^\dagger) + \alpha_2(a_{n+1} + a_{n+1}^\dagger) \right) \cdot h_n + \sum_{n=0}^{N-1} \left[\omega(a_n^\dagger a_n + a_{n+1}^\dagger a_{n+1}) - \omega_1(a_n^\dagger a_{n+1} + a_{n+1}^\dagger a_n) - \omega^+(a_n^\dagger a_{n+1}^\dagger + a_{n+1} a_n) \right], \quad (2)$$

where $h_n = \tilde{C} + S_n^z S_{n+1}^z - (S_n^+ S_{n+1}^- + S_n^- S_{n+1}^+)/2$ and a_n (a_n^\dagger) are phonon annihilation (creation) operators. From Eq. (2) one recovers the spin-Peierls model Eq. (1) if one sets

$$\lambda/\sqrt{2} = \alpha_1 = -\alpha_2, \quad \omega_0 = \omega = 2\omega_1 = 2\omega^+ \quad (3)$$

and $\tilde{C} = 0$, $\tilde{J} = J$. However, as a finite $\tilde{C} < -1/4$ is required for the implementation of the SSE^{13,14} we shift (following Ref. 3) the boson operators a_n and \tilde{J} ,

$$a_n \rightarrow a_n - (C/2)(\alpha_1 + \alpha_2)/(\omega - \omega_1 - \omega^+) \quad (4)$$

$$\tilde{J} \rightarrow \tilde{J} + (\alpha_1 + \alpha_2)^2 C / (\omega - \omega_1 - \omega^+) \quad (5)$$

so that $\tilde{C} = C$, $\tilde{J} \neq J$. Still, to sample the Hamiltonian Eq. (2) with the SSE we have to meet the requirement that all matrix elements of H are negative,^{13,14} implying $\alpha_1 > 0, \alpha_2 > 0, \tilde{J} > 0$, or explicitly ($C = -1/4$):

$$(\alpha_1 + \alpha_2)^2 / 4 \leq \omega - \omega_1 - \omega^+, \quad \alpha_1, \alpha_2 \geq 0. \quad (6)$$

The conditions in Eq. (6) thus forbid a direct analysis of the spin-Peierls Hamiltonian Eq. (1) as may be seen from Eq. (3). However, as we will see we find two scaling laws which enable us to make predictions for the spin-Peierls model Eq. (1).

We define the operators j_n and P_m ,

$$j_n = \frac{iJ_x e}{2\hbar} (S_n^+ S_{n+1}^- - S_n^- S_{n+1}^+) \quad P_m = e \sum_{n>m} S_n^z,$$

which are the current operator for magnetic moments at site n (we denote the ‘‘charge’’ quantum by e in analogy to the electric current) and the potential operator of a local ‘‘voltage drop’’ at site m , respectively. The spin conductance g is the linear response of the operator j_n to the perturbation P_m ,

$$g := \lim_{z \rightarrow 0} \text{Re} \int_0^\infty e^{izt} \frac{i}{\hbar} \langle [j_x(t), P_y] \rangle dt.$$

It is independent of n or m and will be evaluated according to Ref. 9 while the SSE method for the Hamiltonian Eq. (2) is implemented following Refs. 3,11. Note that we are considering only low temperatures and the effect of leads on the conductance is not included.

For the update of the spin degrees of freedom we use the very efficient scheme of ‘‘operator-loop updates’’.¹⁴ The simplest version of an update for the phonons is to suggest a specific change in the configuration and accept/reject it with a certain probability. Here we want to emphasize that we obtain smaller autocorrelation times by using an appropriate cluster update scheme, reminiscent of the loop update (see appendix, section A).

In our simulations we use a system size $N = 192$, a temperature $T = 0.02J/k_B$ and typically perform $2 \cdot 10^5$ MC sweeps.

It should also be mentioned that in our simulations there is no need to introduce a bound for the phonon occupation number, but for technical reasons we impose a restriction of maximum 48 phonons per site; since it is much larger than the phonon numbers created during the simulation this introduces no further error.

Optical Phonons — The two parameters ω_1 and ω^+ lead to a nontrivial dispersion relation of the phonon modes. For the moment we will set them to zero and consider phonons of constant frequency ω . This (Einstein) model was discussed for $\alpha_1 = -\alpha_2$ using the DMRG

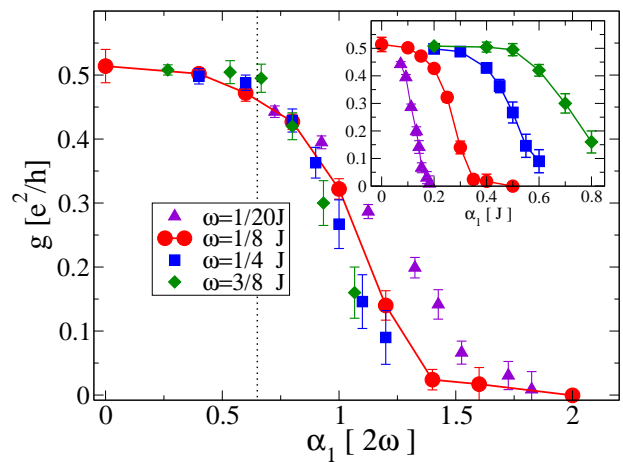


FIG. 1: The conductance as a function of α_1 for various $\omega < J$ for optical phonons ($\omega_1 = 0 = \omega^+$ and $\alpha_2 = 0$). α_1 is given in units 2ω . The dotted line is situated at the critical coupling of Ref. 11. The inset shows the same curves with α_1 in units of J .

method¹⁵ and for $\alpha_2 = 0$ with the SSE.¹¹ Both find that if α_1 is larger than a critical coupling α_c the system undergoes a dimerization transition. In Ref. 15 the authors analyze different values for ω finding that α_c is approximately linear in ω if $\omega < J$. The authors in Ref. 11 discuss only one phonon frequency, namely $\omega = J/8$. They find that $\alpha_c = 1.3\omega$. (Data in our notation.) We will use this result since we focus on $\omega < J$. The reason for this is that in many materials of actual interest J is significantly larger than the Debye temperature; we also find that our QMC method converges better for small ω .

For the conductance $g(T = 0)$ we expect the form of a step function: Above the critical coupling $\alpha_1 > \alpha_c$ it is zero due to the opening of the gap; for $\alpha_1 < \alpha_c$ the system is supposed to be in a Luttinger phase, where the conductance is given by the Luttinger parameter K . Since the Hamiltonian Eq. (2) is spin-rotationally invariant, the latter is fixed to the value of $1/2$ (see Ref. 16).

The fact that g should be constant for $\alpha_1 \leq \alpha_c$ is consistent with an effective Hamiltonian that we can derive using second order perturbation theory (cf. Refs. 15,17)

$$H = \sum_n \left(1 + \frac{\alpha_1^2 + \alpha_2^2}{4\omega} \right) \mathbf{S}_n \cdot \mathbf{S}_{n+1} - \frac{\alpha_1 \alpha_2}{4\omega} \mathbf{S}_n \cdot \mathbf{S}_{n+2}. \quad (7)$$

Indeed, for $\alpha_2 = 0$ we find no change in the conductance to order α_1^2 since g does not depend on the bandwidth J .

In Fig. 1, we present results for the spin conductance g for $\omega_1 = 0 = \omega^+$ and $\alpha_2 = 0$. Within error bars we confirm the expectation that the conductance remains at $1/2$ until the critical coupling is reached. In the gapped phase the conductance goes rather smoothly to zero instead of step-like which is due to the finite temperature $T = 0.02J$ we are using. The point where the conductance has decayed to zero gives a rough estimate for the

coupling α_T where the gap satisfies $\Delta(\alpha_T) = k_B T$. (This can be tested using data from Ref. 15, if we assume that $\Delta(\alpha_1, \alpha_2) = \Delta(\alpha_1 - \alpha_2)$ —which is a natural assumption since this is the scaling relation of α_c to be derived below, cf. Eq. (13). For $\omega = J/20$ we find $\alpha_{T=0.02J} - \alpha_c \approx 0.088J$, i.e., $(\alpha_{T=0.02J} - \alpha_c)/\omega^{0.73} \approx 0.784$ to be compared with Fig. 2 below.)

Subsequent calculations we performed for $T = 0.01J$ find an increased statistical error, but reveal no temperature dependence which implies that $\alpha_{T=0.01J}$ and $\alpha_{T=0.02J}$ are very close to each other. Note that the gap has a typical Kosterlitz-Thouless form:¹⁵ first it opens very slowly, but then it grows rather rapidly.

Since $g(T = 0)$ is a step function—which is fully described by the critical coupling where the conductance drops to zero—it inherits the scaling law of α_c :

$$g(\alpha_1, \omega) = g(\alpha_1/\omega) \quad \text{for } T = 0. \quad (8)$$

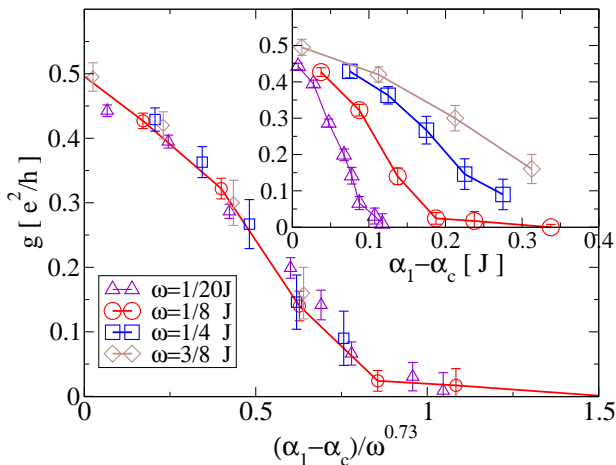


FIG. 2: The conductance as a function of $(\alpha_1 - \alpha_c)/\omega^{0.73}$. The inset shows the same data as a function of $\alpha_1 - \alpha_c$ in units of J .

To analyze the behavior of g in the gapped region more closely, it is instructive to plot g versus $\alpha_1 - \alpha_c$. This is done in Fig. 2. We find good agreement with another scaling relation—different from Eq. (8)—specific to the gapped phase, namely,

$$g(\alpha_1, \omega) = g[(\alpha_1 - \alpha_c)/\omega^\kappa]. \quad (9)$$

where $\kappa = 0.73 \pm 0.05$. It is natural to assume that in the gapped region g depends on the parameters of the system only through $\beta\Delta$. This would in turn imply that the scaling relation Eq. (9) holds for the gap Δ . Note that this relation is not consistent with the exponential behavior of Δ typical for a Kosterlitz-Thouless transition. However, we should expect Eq. (9) to be approximately valid for not too large α and ω . We note that the data for $\Delta(\omega = 0.05, 0.5)$ from Ref. 15 show also good agreement with Eq. (9) when $\kappa = 0.6$.

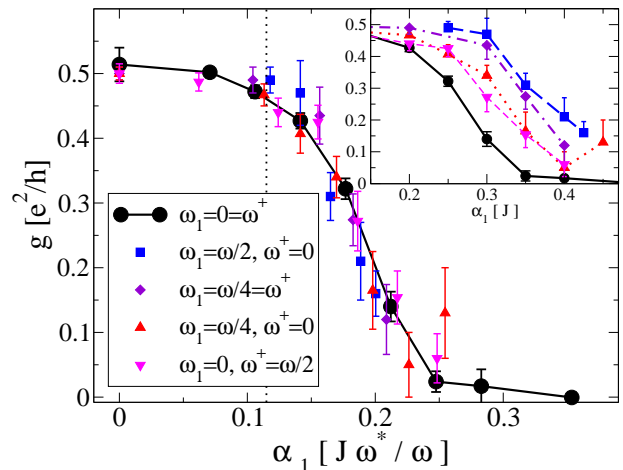


FIG. 3: The conductance as a function of α_1 (in units of $J\omega^*/\omega$) ($\alpha_2 = 0$, $\omega = J/8$) for various dispersions $\omega(k)$. The dotted line indicates the critical coupling of Ref. 11. The inset shows the same data when α_1 is given in units of J .

Acoustical phonons — Now we will consider nontrivial phonon dispersions, $\omega_1 \neq 0 \neq \omega^+$. Performing a canonical Bogoliubov transformation in momentum (k -) space, we obtain the phonon frequency dispersion

$$\omega(k) = 2\sqrt{[\omega - \omega_1 \cos(k)]^2 - [\omega^+ \cos(k)]^2}. \quad (10)$$

We see that if $\omega = \omega_1 + \omega^+$, as, e.g. in the spin-Peierls model Eq. (1), $\omega(k = 0) = 0$, whereas if $\omega > \omega_1 + \omega^+$ there is a gap in the spectrum. This dispersion is illustrated in Fig. 4.

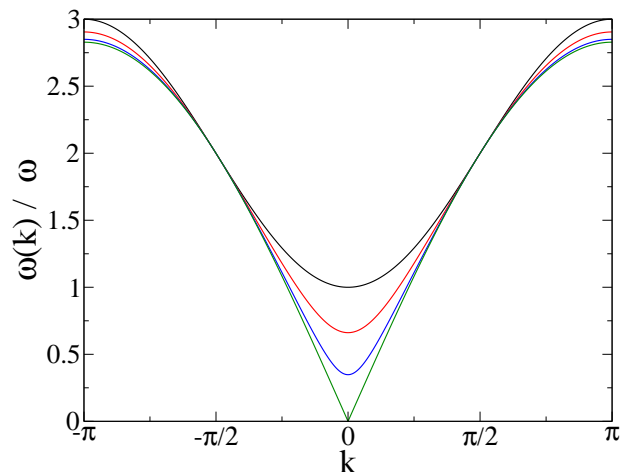


FIG. 4: The phonon dispersion Eq. (10) for $\omega_1 = \omega/2$ and ω^+ is 0, $(3/4)\omega_1$, $(15/16)\omega_1$, ω_1 (from top to bottom). At $\omega^+ = 0$ the parameter ω_1 gives the width of the dispersion and ω its mean value.

After diagonalizing the phonon part of the Hamiltonian Eq. (2) we proceed similarly with the spin-phonon coupling term. To this end, adopting for convenience a

fermion representation ($\mathbf{S}^+ \mapsto c_n^\dagger$) by the Jordan and Wigner transformation, the phonon-fermion scattering term

$$\frac{\alpha_1}{2} \sum_n c_n^\dagger c_{n+1} (a_n + a_n^\dagger)$$

is written in k-space as

$$\frac{\alpha_1}{2} \sum_{k,q} \frac{\sqrt{\omega(k-q)/N} \exp(-iq)}{\sqrt{2\omega - 2\cos(k-q)[\omega_1 + \omega^+]}} c_k^\dagger c_q (a_{k-q} + a_{q-k}^\dagger).$$

Since we are here interested only in the low temperature regime we may assume that the variables k, q lie at the Fermi momenta $\pm\pi/2$. The process responsible for the decrease of the conductance should then be the scattering between two Fermi points by a phonon with momentum π and the only relevant frequency should be $\omega(\pi)$. Thus, for a general dispersion relation, we should recover the same result for g as for the optical phonons of the previous section, by mapping $\omega \rightarrow \omega(\pi)/2$, $\alpha_1 \rightarrow \alpha_1 \sqrt{\omega(\pi)}/\sqrt{2(\omega + \omega_1 + \omega^+)}$. We expect then the conductance g to depend only on α_1/ω^* with $\omega^* = \sqrt{(\omega + \omega_1 + \omega^+)\omega(\pi)}$; to verify this expectation we show g in Fig. 3 for a set of parameters $\omega, \omega_1, \omega^+$ compatible with Eq. (6).

The figure indeed suggests that $g(\alpha_1, \omega, \omega_1, \omega^+) = g(\alpha_1 \omega / \omega^*, \omega)$ and together with Eq. (8) we arrive at the desired scaling relation

$$g(\alpha_1, \omega, \omega_1, \omega^+) = g(\sqrt{2}\alpha_1/\omega^*), \quad \text{for } T = 0. \quad (11)$$

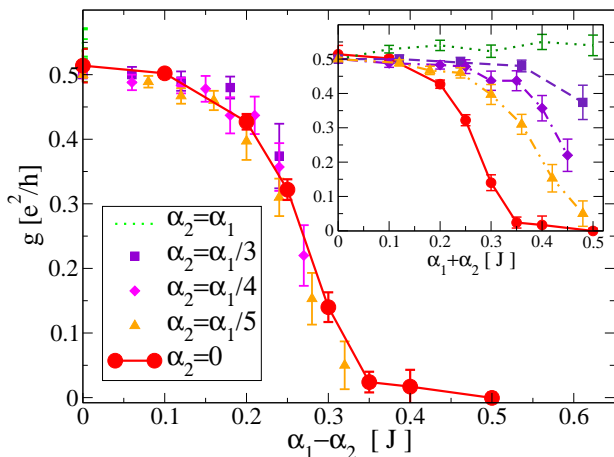


FIG. 5: The conductance as a function of $\alpha_1 - \alpha_2$ for various α_2/α_1 . (The inset shows g vs $\alpha_1 + \alpha_2$. The order of the curve -top to bottom- is the same as in the legend.) Here $\omega = J/8$, $\omega_1 = 0 = \omega^+$, $T = 0.02J/k_B$.

Scaling with α_1 and α_2 — Let us again consider the Hamiltonian in k-space as in the previous section. If we have α_1 and α_2 different from zero, the coupling terms read

$$\frac{1}{2} \sum_{k,q} A_{k,q} (\alpha_1 + e^{i(k-q)} \alpha_2) c_k^\dagger c_q (a_{k-q} + a_{q-k}^\dagger). \quad (12)$$

Here $A_{k,q}$ is a prefactor—whose precise form is for the following discussion irrelevant. At low temperatures we have again $k, q = \pm\pi/2$ which implies that $k - q = 0, \pi$. Hence only two phonon modes are important: $\omega(0)$ and $\omega(\pi)$. The $\omega(0)$ mode describes scattering on one Fermi point which means that it probably rescales the parameters of the system, but has otherwise no influence on the transition. For the phase transition only the $\omega(\pi)$ mode is important. As we see from Eq. (12) the mode with $\omega(0)$ couples to the spin degrees of freedom via $\alpha_1 + \alpha_2$ and the mode $\omega(\pi)$ via $\alpha_1 - \alpha_2$. As the decay of the conductance is due to the opening of the gap, we are led to assume that g depends on $\alpha_1 - \alpha_2$, but not on $\alpha_1 + \alpha_2$, i.e.,

$$g(\alpha_1, \alpha_2) = g(\alpha_1 - \alpha_2). \quad \text{for } T = 0 \quad (13)$$

(Alternatively, one can motivate this scaling law with a Mean Field Theory ansatz which is outlined in the appendix, section C.)

In Fig. 5 we confirm this scaling by the overlap of curves as a function of $\alpha_1 - \alpha_2$, while in the inset we indeed find that the dimerization transition is delayed by increasing α_2/α_1 , till $\alpha_2 = \alpha_1$ where it is absent as predicted by Eq. (13).

A further test of Eq. (13) is provided by comparing data for α_c . For $\omega = J/8$ and $\alpha_2 = 0$ Ref. 11 finds $\alpha_c = 0.163J$ (with 4% uncertainty), whereas according to Ref. 15 for the same ω but $\alpha_1 = -\alpha_2$ the transition occurs when $\alpha_1 - \alpha_2 = 0.176J$. The difference of the two values is 8% which means reasonable agreement.

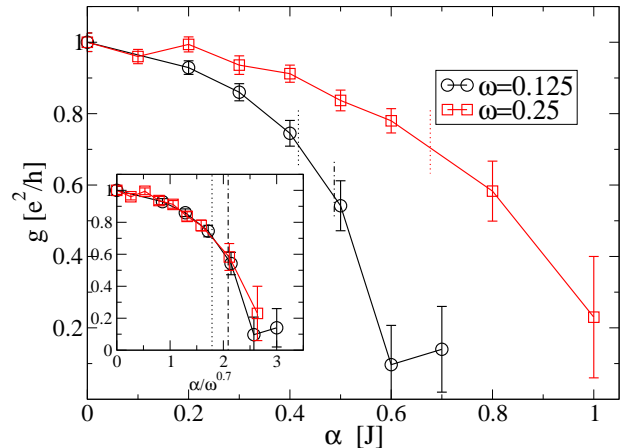


FIG. 6: The conductance of the XY model as a function of α_1 ($\alpha_2 = 0$) for two ω (here $T = 0.01J$). The dotted line gives the critical coupling if one assumes that the scaling law $\alpha_c(\alpha_1, \alpha_2) = \alpha_c(\alpha_1 - \alpha_2)$ holds. The dot-dashed line gives the critical α_c extracted from Fig. 8.

XY model— In this section we turn to the XY model, that is we replace $\mathbf{S}_n \cdot \mathbf{S}_{n+1}$ in the Hamiltonian Eq. (2) by $S_n^x S_{n+1}^x + S_n^y S_{n+1}^y$. The model was studied by Caron and Moukouri¹⁸ for $\alpha_1 = -\alpha_2$. They found a phase transition similar to the one in the spin-Peierls model but

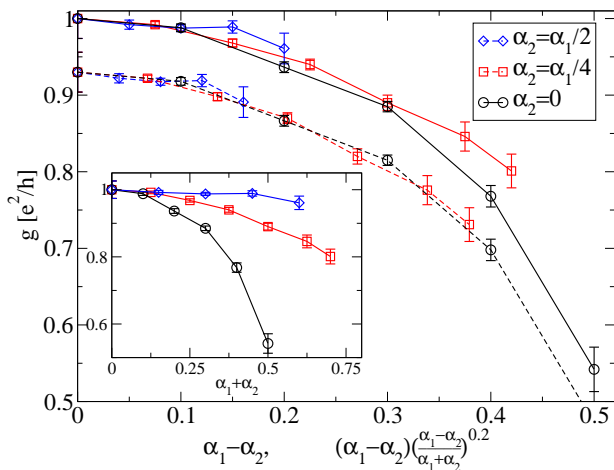


FIG. 7: The conductance of the XY model as a function of $\alpha_1 - \alpha_2$ (solid curves), $(\alpha_1 - \alpha_2)^{1.2}/(\alpha_1 + \alpha_2)^{0.2}$ (dashed curves which are offset by -0.07 for clarity) and $\alpha_1 + \alpha_2$ (inset) for various α_2/α_1 with $\omega = J/8, T = 0.01J$.

here $\alpha_c \propto \omega^{0.7}$. We computed the conductance for two phonon frequencies. The results are shown in Fig. 6. We find that the zero temperature conductance obeys the scaling law

$$g(\alpha_1, \omega) = g(\alpha_1/\omega^{0.7}). \quad (14)$$

It is important to point out that the XY model is not spin-rotationally invariant and therefore the value of the conductance is not fixed in the Luttinger phase, but rather decreases monotonously, as the Fig. 6 shows. In the gapped phase the conductance decays again quite smoothly to zero, such that it is barely possible to decide where exactly the transition takes place.

We therefore employed here two different methods for calculating α_c . First QMC simulations for the staggered kinetic energy which give a rigorous upper bound (details are deferred to the appendix, section B), second we used the data for α_c from Ref. 18 while assuming that the scaling law Eq. (13), $g(\alpha_1, \alpha_2) = g(\alpha_1 - \alpha_2)$, holds

The two results for α_c are indicated by lines in Fig. 6 for comparison. The difference between the two predictions for α_c is about 15%. One should emphasize again that both methods are not numerically exact: the QMC yields only an upper bound for α_c , and the other method relies on the validity of Eq. (13) which is examined in Fig. 7 by considering nonzero α_2 . For the parameter accessible to us Eq. (13) seems to be approximately, but *not exactly* fulfilled.

In the Heisenberg model the dependence on α_1, α_2 and ω was described by two separate scaling laws Eqs. (8) and (13). For the XY model the situation is more complicated, as we found that for $\alpha_2 = \alpha_1/4$ the scaling law Eq. (14) is violated. This implies that a generalization of Eq. (13) which holds for the XY model must depend on ω . We will not try to find such a generalization here, but want to point out that for the special

case of $\omega = J/8$ one can obtain a much better fit for our data (for $\alpha_2/\alpha_1 = 0, 0.25, 0.5$) than Eq. (13) by using the following modified scaling ansatz (see Fig. 7)

$$g(\alpha_1, \alpha_2) = g \left[(\alpha_1 - \alpha_2) \left(\frac{\alpha_1 - \alpha_2}{\alpha_1 + \alpha_2} \right)^{0.2} \right].$$

Conclusions — We have shown that the known scaling laws for α_c in the Heisenberg and the XY model, i.e., Eqs. (8) & (14) also hold for the conductance. For the spin-rotationally invariant case we found a generalization for acoustic phonons Eq. (11) as well as a scaling relation for the gap Eq. (9). We also discussed the difference between two possible couplings to phonons ($\alpha_2 = 0$ & $\alpha_2 = -\alpha_1$). For the spin-rotationally invariant case the two ways of coupling are related by a simple scaling law Eq. (13), whereas for the XY chain the situation appears to be more complicated. Assuming that our scaling laws are not restricted we may make a prediction for the conductance of the spin-Peierls model Eq. (1) by putting together Eqs. (3), (11) and (13) as well as data for the critical coupling from Ref. 11. We expect a step-like conductance which drops to zero when $\lambda = 0.65 \cdot 2^{5/4} \omega_0 \approx 1.55 \omega_0$.

One final comment should be made. Over the last few years, it has generally agreed upon that the conductance measured in experiments corresponds to the conductance of a system coupled to noninteracting leads. The leads - which were not considered here - may strongly affect the conductance.^{19,20} We can argue however that the dimerization transition we observed will drive the conductance to zero even if it occurs only locally, i.e. in the interacting part system and not in the leads. Hence, we think that our results have a clear experimental consequence.

We would like to acknowledge useful discussions with D. Baeriswyl and financial support by the E.U. grant MIRG-CT-2004-510543.

APPENDIX A: MC UPDATE FOR THE PHONONS

We write the Hamiltonian Eq. (2) in the form $H = \sum h_n^{(i,j,k)}$, where n is the site (bond) index and indices (i, j, k) denote different types of (local) operators.

The parameter j (resp. k) assumes values from -1 to 1 and refers to the change of the phonon number on site n (resp. $n + 1$) resulting from the action of the operator $h_n^{(i,j,k)}$. In the sequel we will refer to j or k as phonon parameters. The index i refers to the action on the spin degrees of freedom. For example, the operators for different i and $j = 0 = k$ read

$$\begin{aligned} h_n^{(1,0,0)} &= JS_n^+ S_{n+1}^- / 2 & h^{(2,0,0)} &= \left(h^{(1,0)} \right)^\dagger \\ h^{(3,0,0)} &= C + JS_n^z S_{n+1}^z + \omega (a_n^\dagger a_n + a_{n+1}^\dagger a_{n+1}). \end{aligned}$$

Following Ref. 13, we expand the Boltzmann weight in terms of the local operators, i.e., we sample the operator strings $\prod_l^m \langle l|h(l)|l+1 \rangle$ according to their weight in the Boltzmann factor ($|l \rangle$ are states in the S^z -phonon occupation-number basis and $h(l)$ is the local operator $h_n^{(i,j,k)}$ which appears on the l th position of the string). The spin degrees of freedom can be updated using the very efficient scheme of operator loops.¹⁴ During this update the parameters j and k remain unchanged. All that remains to be done is to devise an additional update for the phonon parameters.

This is achieved as follows: As the operators a_n and a_n^\dagger appear always pairwise in the string, we have to increase the phonon parameter at one position (of the string) and decrease it at another position. In principle the two positions can be chosen at random, but here we want to point out that this can be done more efficiently: We choose an operator $h_n^{(i,j,k)}$ in the string. Next, we decrease (resp. increase, depending on an appropriate probability) one of its phonon parameters (associated with a site which we will call m). For the previous (resp. next) operator in the string we choose—with a certain probability—one of three options: either (i) we update the phonon number on site m by +1 or (ii) we cancel the operation and restore the initial configuration, or (iii) we increase (resp. decrease) the phonon parameter related with site m . In case (ii) or (iii) the procedure stops, while in the first case it is iterated until we finally choose one of the other options.

Even though one might suspect that because of option (ii) the algorithm is inefficient—since it is reminiscent of the bounce process in Ref. 14—we find that our new update scheme reduces the autocorrelation time significantly. The reason for the latter may be seen in the fact that we choose only one position of the two phonon operators at random, the other is—in some optimized way—chosen by the MC algorithm.

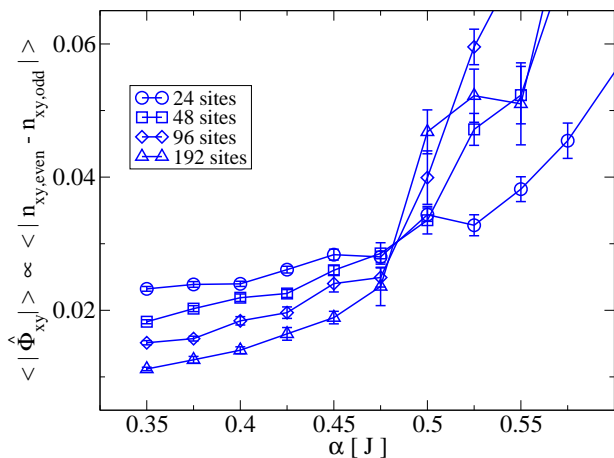


FIG. 8: Absolute value of the contributions of the staggered kinetic energy $\langle |\hat{\Phi}_{xy}| \rangle$ (see text) for the XY-model with $\omega = J/8$ at $T = 0.01J$. Here we use periodic boundary conditions and 10^4 MC sweeps.

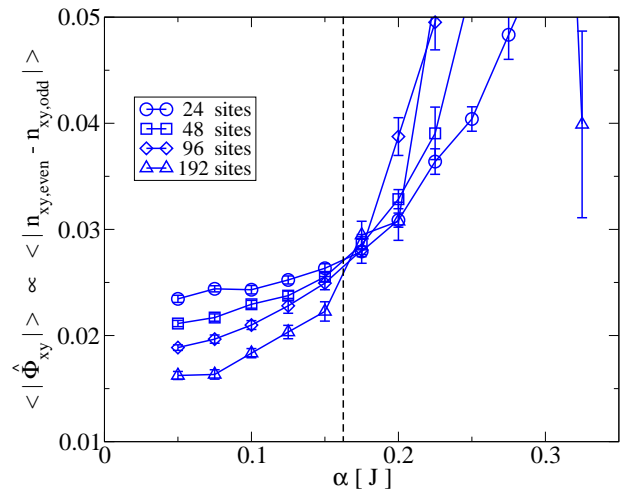


FIG. 9: Absolute value of the contributions of the staggered kinetic energy $\langle |\hat{\Phi}_{xy}| \rangle$ (see text) for the Heisenberg-model with $\omega = J/8$ at $T = 0.01J$. The dashed line give the critical coupling from Ref. 11. Here we use periodic boundary conditions and 10^4 MC sweeps.

APPENDIX B: EVALUATION OF THE CRITICAL COUPLING WITH QMC

The simplest method to determine α_c with Monte Carlo is measuring the order parameter. In our case we have two options for the order parameter: one is

$$\Phi_a = \sum_n (-1)^n (a_n + a_n^\dagger) / N$$

the staggered bond length,²¹ another is the staggered kinetic energy²²

$$\Phi_{xy} = \sum_n (-1)^n (S_n^+ S_{n+1}^- + S_n^- S_{n+1}^+) / (2N).$$

Since these operators are linear combinations of terms appearing in the Hamiltonian, there is a simple method to evaluate the expectation values with the SSE.¹³ To this end we define $n_{a,n}$ (and $n_{xy,n}$) which are the sum of the numbers of appearances of the operators $C a_n$ and $C a_n^\dagger$ ($J/2 S_n^+ S_{n+1}^-$ and $J/2 S_n^- S_{n+1}^+$) in the string of operators created and updated in the simulation process. The expectation values of the order parameters are related with the mean values of the numbers $n_{a,n}$ and $n_{xy,n}$; the relation being

$$\langle \Phi_a \rangle = \sum_n (-1)^n \langle -n_{a,n} \rangle / (N\beta C)$$

and

$$\langle \Phi_{xy} \rangle = \sum_n (-1)^n \langle -n_{xy,n} \rangle / (N\beta \tilde{J}).$$

Since the contributions to the order parameters may be positive or negative, it is difficult to detect a finite

dimerization—especially, when we are close to the critical coupling. Hence, it is difficult to decide whether we are in the gapped phase or not. We therefore calculate the following expectation values

$$\langle |\hat{\Phi}_a| \rangle = \left\langle \left| \sum_n (-1)^n n_{a,n} \right| \right\rangle / (N\beta C)$$

and

$$\langle |\hat{\Phi}_{xy}| \rangle = \left\langle \left| \sum_n (-1)^n n_{xy,n} \right| \right\rangle / (N\beta\tilde{J}).$$

(One should note that in general $\langle |\hat{\Phi}_a| \rangle \neq \langle |\Phi_a| \rangle$ where $|\Phi_a| = \sqrt{\Phi_a^2}$.) These have non-zero values, but in the gapless phase they should go to zero in the thermodynamic limit. We note that while $\langle \Phi_a \rangle$ is independent of C the expectation value $\langle |\hat{\Phi}_a| \rangle$ *does* depend on the shift C . Because of this and the fact that $\langle |\hat{\Phi}_a| \rangle > \langle |\hat{\Phi}_{xy}| \rangle$ (which suggests that $\langle |\hat{\Phi}_{xy}| \rangle$ decays faster with N) we prefer the second order parameter to the first and will only discuss $\langle |\hat{\Phi}_{xy}| \rangle$.

Results for $\langle |\hat{\Phi}_{xy}| \rangle$, the staggered kinetic energy, are presented in Figs. 8 and 9. For the XY model (Fig. 8) the order parameter $\langle |\hat{\Phi}_{xy}| \rangle$ decreases with system size as long as $\alpha_1 \leq 0.475J$. For $\alpha_1 \geq 0.5J$ it seems to increase with system size rather than decrease. We conclude that $\alpha_c < 0.5J$. A correct assessment of the critical coupling remains difficult. A rough estimate for α_c is obtained by assuming that α_c lies in the interval $0.475J < \alpha_1 < 0.5J$ where the behavior of $\langle |\hat{\Phi}_{xy}| \rangle$ changes. This yields $\alpha_c \approx 0.4875J \pm 0.0125J$. In principle, this estimate gives only an upper bound for α_c , but when we apply the same method to the spin-rotationally invariant case, we find

good agreement with the value for α_c from Ref. 11 (see Fig. 9).

APPENDIX C: MEAN FIELD

To better understand the physics of the model a mean field analysis is helpful. The main idea is to replace the displacements $(a_n + a_n^\dagger)/\sqrt{2}$ by classical variables x_n . A common but general ansatz for these variables is $x_n = \bar{x} + (-1)^n \Delta$. Substituting this ansatz into the Hamiltonian Eq. (2) we obtain,

$$H_{MF} = \sum_n J_n S_n \cdot S_{n+1} \quad (C1)$$

$$J_n = J + \sqrt{2}(\alpha_1 + \alpha_2)\bar{x} + (-1)^n \sqrt{2}(\alpha_1 - \alpha_2)\Delta.$$

One sees that the spin-Peierls model Eq. (1) does not depend on \bar{x} because of $\alpha_1 = -\alpha_2$. At the mean field theory level we arrive at two conclusions, (i) there is a shift in J proportional to $(\alpha_1 + \alpha_2)$ and (ii) there is a dimerization transition where the dimerization is proportional to $(\alpha_1 - \alpha_2)$. In the spin-Peierls model ($\alpha_1 = -\alpha_2$) the shift in J is absent, whereas in a toy model with $\alpha_1 = \alpha_2$ no dimerization should be found. In our simulations ($\alpha_1, \alpha_2 \geq 0$) we always have a shift but, since the conductance at $T = 0$ does not depend on J , we expect that g is independent of $\alpha_1 + \alpha_2$ and we arrive at the scaling law

$$g(\alpha_1, \alpha_2) = g(\alpha_1 - \alpha_2). \quad (C2)$$

-
- ¹ S.A. Wolf et al., *Science* **294**, 1488 (2001).
² M.C. Cross and D.S. Fisher, *Phys. Rev.* **B19**, 402 (1979).
³ A.W. Sandvik, R.P.R. Singh, and D.K. Campbell, *Phys. Rev.* **B56**, 14510 (1997).
⁴ A.V. Sologubenko, K. Giannò, H.R. Ott, A. Vietkine and A. Revcolevschi, *Phys. Rev.* **B64**, 054412 (2001).
⁵ C. Hess, C. Baumann, U. Ammerahl, B. Büchner, F. Heidrich-Meisner, W. Brenig and A. Revcolevschi, *Phys. Rev.* **B64**, 184305 (2001).
⁶ X. Zotos and P. Prelovšek, in *Interacting Electrons in Low Dimensions*, Kluwer Academic Publishers (2003); arXiv:cond-mat/0304630.
⁷ J.V. Alvarez, C. Gros, *Phys. Rev. Lett.* **88**, 077203 (2002); *Phys. Rev.* **B66**, 094403 (2002).
⁸ F. Heidrich-Meisner, A. Honecker, D.C. Cabra, and W. Brenig, *Phys. Rev.* **B68**, 134436 (2003).
⁹ K. Louis and C. Gros, *Phys. Rev.* **B68**, 184424 (2003); K. Louis, Ph.D. thesis, University of Saarbrücken, (2004).
¹⁰ F. Meier and D. Loss, *Phys. Rev. Lett.* **90**, 167204 (2003).
¹¹ A.W. Sandvik and D. Campbell, *Phys. Rev. Lett.* **83**, 195 (1999).
¹² R.W. Kühne and U. Löw, *Phys. Rev.* **B60**, 12125 (1999).
¹³ A.W. Sandvik, *Phys. Rev.* **B59**, R14157 (1999).
¹⁴ O.F. Syljuåsen and A.W. Sandvik, *Phys. Rev.* **E66**, 046701 (2002).
¹⁵ R.J. Bursill, R.H. McKenzie, and C.J. Hamer, *Phys. Rev. Lett.* **83**, 408 (1999).
¹⁶ H.J. Schulz, G. Cuniberti, and P. Pieri in *Field Theories for Low-Dimensional Condensed Matter Systems*, G. Morandi et al. Eds. Springer (2000).
¹⁷ K. Kuboki and H. Fukuyama, *J. Phys. Soc. Jpn.* **56**, 3126 (19987); G.S. Uhrig, *Phys. Rev. B* **57**, R14004 (1998).
¹⁸ L.G. Caron and S.Moukouri, *Phys. Rev. Lett.* **76**, 4050 (1996).
¹⁹ I. Safi and H.J. Schulz, *Phys. Rev. B* **52**, R17040 (1995).
²⁰ D.L. Maslov and M. Stone, *Phys. Rev. B* **52**, R5539 (1995).
²¹ C. Raas, U. Löw, G.S. Uhrig, and R.W. Kühne, *Phys. Rev. B* **65**, 144438 (2002).
²² P. Sun, D. Schmeltzer, and A.R. Bishop, *Phys. Rev. B* **62**, 11308 (2000).